

Detecting the quantum critical point in high-temperature superconducting cuprates via complex network theory

Andrey A. Bagrov^{1,*,\dagger}, Mikhail Danilov^{2,\dagger}, Sergey Brener², Malte Harland², Alexander I. Lichtenstein²
& Mikhail I. Katsnelson¹

¹*Radboud University, Institute for Molecules and Materials, 6525AJ Nijmegen, The Netherlands*

²*Institute of Theoretical Physics, University of Hamburg, 20355 Hamburg, Germany*

**Email: abagrov@science.ru.nl*

\dagger These authors equally contributed

The current understanding of high- T_c superconductivity in cuprates assumes a crucial role of strong electron correlations¹⁻⁴. There is a popular view that a single-band $t - t'$ Hubbard model⁵ is the minimal model to catch the main relevant physics but even this oversimplified model is too complicated to be treated accurately and convincingly. It has been thoroughly studied numerically, and a number of valuable results have been obtained⁶⁻¹¹. On the other hand, a considerable success in phenomenological description of high- T_c superconductors has been achieved within the paradigm of Quantum Critical Point^{12,13} (QCP) - a parental state of a variety of exotic phases that is characterized by dense entanglement and absence of well-defined quasiparticles. However, the microscopic origin of the critical regime in real materials remains an open question. Here, we suggest that emergence of the QCP is tightly connected with entanglement in real space and identify its location on the phase diagram of the hole-doped $t - t'$ Hubbard model. To detect the QCP we study a weighted graph of

inter-site quantum mutual information within a four-by-four plaquette that is solved by exact diagonalization. We demonstrate that certain characteristics of such a graph, viewed as a complex network, exhibit peculiar behavior around a point on the phase diagram corresponding to the onset of pseudogap in $\text{YBa}_2\text{Cu}_3\text{O}_7$. This method allows us to overcome difficulties caused by finite size effects and to identify the transition point even on a small lattice, where long-range asymptotics of correlation functions cannot be accessed.

The phenomenon of high-temperature superconductivity (HTSC) still remains very puzzling after more than thirty years since the discovery of superconducting copper-oxide compounds¹⁴. Serious hopes for the understanding of this phenomenon are related to the concept of a quantum critical point (QCP)¹³, - an exotic state of matter that exhibits scale invariance and lacks long-lived quasiparticles, and thus cannot be described by means of conventional Fermi-liquid theory. Contemporary discussions of observed properties of HTSC are frequently organized around this concept^{15,16}. From the theoretical side, focus on QCP requires a change of basic mathematical tools. The diagrammatic approach, the main apparatus of quantum many-body theory during the last sixty years^{17,18}, is very well fitted to the description of quasiparticles; microscopic justification of the Landau Fermi-liquid theory remains probably its main success. A paradigmatic shift in studying strongly coupled systems near the QCP has occurred when it was realized that the anti de Sitter/Conformal field theory (holographic) correspondence¹⁹ can be used to analyze certain universal phenomenological properties of correlated electronic matter in the regime where the traditional Fermi-liquid picture breaks down^{20,21}. With regard to the high-temperature superconductors, this allowed to resolve within a relatively short time frame a number of puzzles that

remained perplexing for decades¹. The correspondence provided an explanation for the linear- T scaling of DC resistivity in the normal state of cuprates²² (known as strange metals), relating it to general hydrodynamic properties of systems with minimal viscosity proportional to the thermodynamic entropy²³. It was shown²⁴ that the Hall angle, - the temperature dependent ratio of the Hall and DC conductivities, $\tanh \theta_H = \sigma_{xy}/\sigma_{xx} \sim 1/T^2$, can be naturally interpreted in terms of a two-constituent quantum liquid, where the regular quasiparticles and the critical sectors give independent contributions to the conductivity, leading to an anti-Matthiessen rule for transport. A new mechanism of the interaction-driven metal-insulator transition that causes anisotropic localization has been suggested²⁵, and it appears to be fully in line with the localization of conducting electron gas in two-dimensional CuO planes, while the conductivity in the orthogonal direction is suppressed. Other phenomena, such as the formation of Fermi arcs seen in the angle-resolved photoemission spectra of high-Tc compounds, or charge density waves also fit pretty naturally into the context of quantum criticality²⁶.

The main problem of this approach is its purely phenomenological character. It cannot explain by itself why the high-Tc compounds, contrary to the most of interesting condensed matter systems, do not behave as the Fermi liquid but instead are characterized by minimal quantum viscosity and other fancy properties. Such an explanation requires an analysis of electronic structure of specific materials.

In an attempt to proceed along this path, we shall focus on a particular minimal model that was formulated⁵ on the basis of the density functional band structure of cuprates, - the single-band

$t - t'$ Hubbard model on a square lattice given by the Hamiltonian

$$H = -t \sum_{\langle i,j \rangle, \sigma} c_{i,\sigma}^\dagger c_{j,\sigma} - t' \sum_{\langle\langle l,k \rangle\rangle, \sigma} c_{l,\sigma}^\dagger c_{k,\sigma} + h.c. + U \sum_i n_{i,\uparrow} n_{i,\downarrow}, \quad (1)$$

where, the first sum is taken over the pairs $\langle i, j \rangle$ of nearest neighbors, the second one - over the pairs $\langle\langle l, k \rangle\rangle$ of next-to-nearest (diagonal) neighbors, $c_{i,\sigma}$ is the electron annihilation operator, and the on-site occupation operator is $n_{i,\sigma} = c_{i,\sigma}^\dagger c_{i,\sigma}$. Correlation effects beyond the band structure approximation in this model have been thoroughly analyzed with different methods, and there are a number of good indications that it captures all the relevant features of cuprate superconductors. In a series of papers²⁷⁻³², perturbative renormalization group studies of the model have been conducted, and the emergence of the superconducting order parameter and the competition between superconductivity and antiferromagnetism were demonstrated. In particular³¹, it was argued that the next-to-nearest neighbor hopping t' plays a crucial role in the stabilization of superconductivity. A complementary approach is based on the cluster dynamical mean-field studies which consider a 2-by-2 plaquette as an elementary unit³³. Recently¹¹, it was noticed that this plaquette has a very special electronic structure for the parameters and the electron occupation number typical for the the optimal doping regime in $\text{YBa}_2\text{Cu}_3\text{O}_7$ ($t'/t = -0.3$, $U/t \simeq 6$), with an “accidental” degeneracy of many-electron energy levels and formation of the soft fermion mode due to this degeneracy. The pseudogap forms via this mode by a mechanism of the Fano antiresonance, and the superconducting d-wave susceptibility dominates over other instability channels. This behavior was interpreted in terms of formation of a local plaquette valence bond state. On a larger scale, the ground state of the model has been analyzed by means of density matrix renormalization group³⁴ (DMRG) (see also³⁵ for the related studies of its cousin, $t - J$ -model), and additional arguments in

favor of stabilization of superconductivity by the next-to-nearest neighbor hopping were provided. In turn, at temperatures above the superconducting phase transition, determinantal Monte Carlo computations³⁶ demonstrated that the DC resistivity exceeds the Mott-Ioffe-Regel limit and scales linearly with temperature.

The search for the QCP in the $t-t'$ Hubbard model has been performed within the dynamical cluster approximation⁸, and its existence has been proven by studying thermodynamics properties of the model at finite temperature and their further extrapolation to $T = 0$. However, it is tempting to get a deeper insight into the microscopics of the QCP and demonstrate its emergence due to interactions of electrons at low temperatures.

Since large scale simulations of the fermionic Hubbard model away from half-filling are challenging because of the sign problem, it is natural to ask whether we can extract any information about the tendency to form critical states out of small cluster solutions obtained by means of exact diagonalization. At first, this goal does not seem realistic since studying systems in the critical regime unavoidably requires dealing with long-range correlations, while all the microscopic precursors of the transition on small lattices would be washed out by the finite-size effects. However, it is useful to bear in mind that, in the context of many-body quantum dynamics, the concept of entanglement and the phenomenon of collective emergence go hand in hand. An archetypical example of such relation is the Cooper pairs in the BCS theory of superconductivity: while the ground state wavefunction has a form of a product state of the Cooper pairs, each pair itself is a two-body entangled system. Therefore it is natural to expect that major transitions in phenomeno-

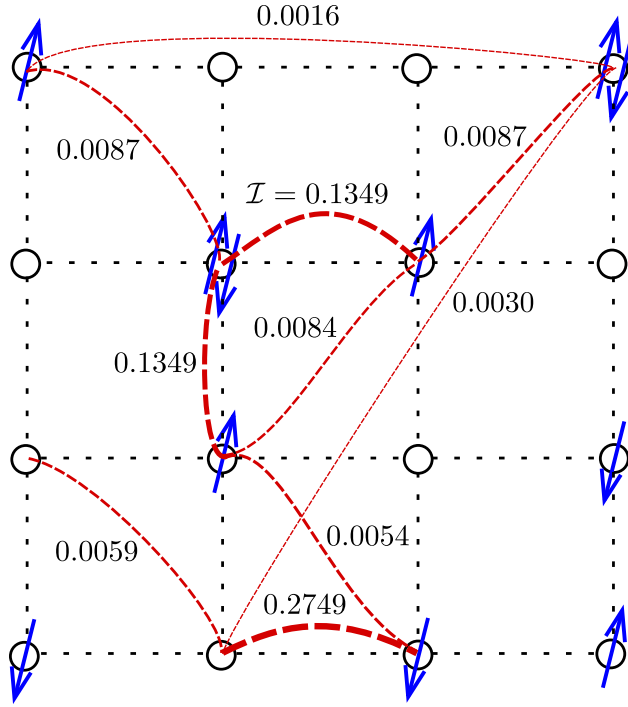


Figure 1: An artistic view of the mutual information complex network defined on the Hubbard lattice. While the network is fully connected, for illustrative purposes, only some of the network links are shown. The shown values of inter-site mutual information correspond to the case of non-periodic boundary conditions, (6, 6) sector, $U = 7.5$.

logical properties of many-body systems would be reflected in the patterns of entanglement, and quantum criticality should leave its fingerprint on all scales, not only in the deep infrared limit.

Recently, a novel approach to phase transitions in quantum lattice models based on complex network theory has been suggested^{37,38}. It was noticed that a particular structure that can be computed with relative ease and appears to be very sensitive to reconfigurations of the quantum state is the network of quantum mutual information. The mutual information between two subsystems

A and B of a larger systems is defined as

$$\mathcal{I}_{AB} = S_A + S_B - S_{A \cup B}, \quad (2)$$

where $S_A = -\text{Tr} \rho_A \log \rho_A$ is the von Neumann entropy, and $\rho_A = \text{Tr}_{\bar{A}} \rho$ is the density matrix of subsystem A . Then we can associate a weighted graph with a state of a quantum lattice system, e.g. the Hubbard model, by considering the lattice sites $i = 1 \dots N$, where N is the number of sites, as nodes of the graph, and the values of pairwise inter-site mutual information I_{ij} play the role of weights on the graph links (see Fig. 1). This representation is appealing for the following reason. Once a wave function on the lattice is known, it is easy to compute the entanglement entropy of a pair of sites and thus the mutual information. At the same time, such a network by design contains information of multi-partite quantum correlations which could be very important to understand the dynamics of strongly correlated systems. In the cases of the 1d Ising model in a transverse field and the 1d Bose-Hubbard model, it was demonstrated that certain characteristics of the mutual information network can be used to detect quantum phase transitions^{37,38}. Namely, behavior of the following functions upon changing parameters of the models has been studied:

- **Clustering** of a weighted graph is defined as

$$C = \frac{\text{Tr} \mathcal{I}^3}{\sum_{j \neq i}^N \sum_{i=1}^N [\mathcal{I}^2]_{ij}}, \quad (3)$$

where N is the total number of sites in the lattice, and \mathcal{I} is the $N \times N$ matrix of inter-site mutual information. One can see that this quantity maximizes on graphs with a lot of three-link loops with high weights. For the cases studied in Ref.³⁷, it was shown that it serves as sensitive detector that exhibits a clear dip at the phase transition point.

- **Disparity** of a single node in a network is defined as a measure to capture how non-uniformly weights on the links attached to this node are distributed:

$$Y_i = \frac{\sum_{j=1}^N (\mathcal{I}_{ij})^2}{\left(\sum_{j=1}^N \mathcal{I}_{ij}\right)^2} \quad (4)$$

For example, if the node has the same value of mutual information with all the other nodes of the network, its disparity would be $Y_i = 1/(N - 1)$, while if it correlates only with one neighbor, the disparity maximizes as $Y_i = 1$. Physically speaking, high disparity of a lattice site means that it tends to correlate only with a few other sites, and “factorize out” of the rest of the system. In the context of quantum many-body physics such a behavior would be typical for states that can be nearly decomposed into product states. On the other hand, low disparity means that the site correlates with a large number of degrees of freedom.

- **Density** is an overall characteristic of a network given by

$$D = \frac{1}{N(N-1)} \sum_{i,j=1}^N \mathcal{I}_{ij}, \quad (5)$$

i.e. it is the averaged fraction of all the weights (mutual information values) of the network.

To gain more intuition on what properties of the many-body quantum state it reflects, we shall estimate an upper bound on this measure. If site i of the network is maximally entangled with the rest of the system, its entanglement entropy equals $S_i = \ln d = \ln 4$, where $d = 4$ is dimension of the local on-site Hilbert space in Hubbard model. On the other hand, mutual information monogamy theorem implies that $S_i \geq \sum_{j \neq i} \mathcal{I}_{ij}$. From that we readily conclude

$$D \leq \frac{1}{N(N-1)} \sum_{i=1}^N S_i \leq \frac{\ln 4}{N-1} \xrightarrow{N \rightarrow \infty} 0 \quad (6)$$

i.e. the mutual information network is generally sparse even if the system is highly entangled. Note that bound (6) can be saturated in physically very distinct cases. D is maximal if either each single site is maximally entangled with just one partner site, and the state as a whole decomposes into a product of Bell pairs, or if the entanglement between the site and the rest of the system is homogeneously scrambled over all the sites. To distinguish between such configurations one has to refer to the disparity which we defined above.

- **Pearson correlations** measure how much two nodes i and j of a network differ from each other:

$$r_{ij} = \frac{\sum_{k=1}^N (\mathcal{I}_{ik} - \langle \mathcal{I}_i \rangle) (\mathcal{I}_{jk} - \langle \mathcal{I}_j \rangle)}{\sqrt{\sum_{k=1}^N (\mathcal{I}_{ik} - \langle \mathcal{I}_i \rangle)^2} \sqrt{\sum_{k=1}^N (\mathcal{I}_{jk} - \langle \mathcal{I}_j \rangle)^2}}, \quad (7)$$

$$\langle \mathcal{I}_i \rangle = \frac{1}{N} \sum_{j=1}^N \mathcal{I}_{ij}$$

In Ref.³⁷ Pearson correlations of neighboring nodes were shown to develop a cusp around the phase transition point.

For one-dimensional Ising and Bose-Hubbard models³⁷, this approach to detecting quantum phase transitions points was successfully applied for systems of $\sim 10^2$ sites, and was demonstrated to be very robust upon finite-size effects. In the two-dimensional case, we are limited by much smaller system sizes (we perform exact diagonalization for a 4-by-4 plaquette), and should not expect our results to be free from finite-size artifacts. Still, as we shall see in the next section, the network measures exhibit clearly distinguishable features at certain values of parameters of the $t-t'$ Hubbard model close to the level-crossing point observed in a 2-by-2 plaquette¹¹.

Results. We have computed the complex network measures discussed above across the space of parameters of the $t - t'$ Hubbard model. We have studied 4-by-4 plaquette adopting both the non-periodic and periodic boundary conditions. We take $t'/t = -0.3$, which is estimated to be the value of next-neighbor hopping in the Hubbard model of YBCO compounds, consider the system in the canonical ensemble, and within each fixed particles number sector compute the network measures scanning over $U \in [0, 12]$. The temperature is fixed to $1/T = \beta = 100$ (all energies are expressed in the units of $|t|$).

We assume that a transition point is evident if all the measures exhibit some clear features around the same point. Accepting this criterion, we can claim with a high confidence that for $t'/t = -0.3$ a phase transition is seen in the $(6, 6)$ quantum number sector (6 electrons with spin up, 6 electrons with spin down), which corresponds to the hole doping of $\delta = 25\%$. Within this sector, there is a point where clustering, density, the Pearson coefficients between neighboring sites, and disparity (the latter – only in the non-periodic case), considered as functions of the Coulomb repulsion U , – all have a clear cusp. Concrete value of Coulomb repulsion U seems to be dependent on the choice of boundary conditions, - it is $U \simeq 7.5$ for the open cluster, and $U \simeq 9.5 - 10$ for the periodic one. That is not unexpected since we perform the small-scale analysis and cannot eliminate the finite-size effects.

At the same time, in the density of states (d.o.s.) the transition point is (almost) invisible. Some minor peculiarity at the quantum critical point is visible in the density of states at $t'/t = -0.3$ for non-periodic boundary conditions. Around the transition point identified by means of

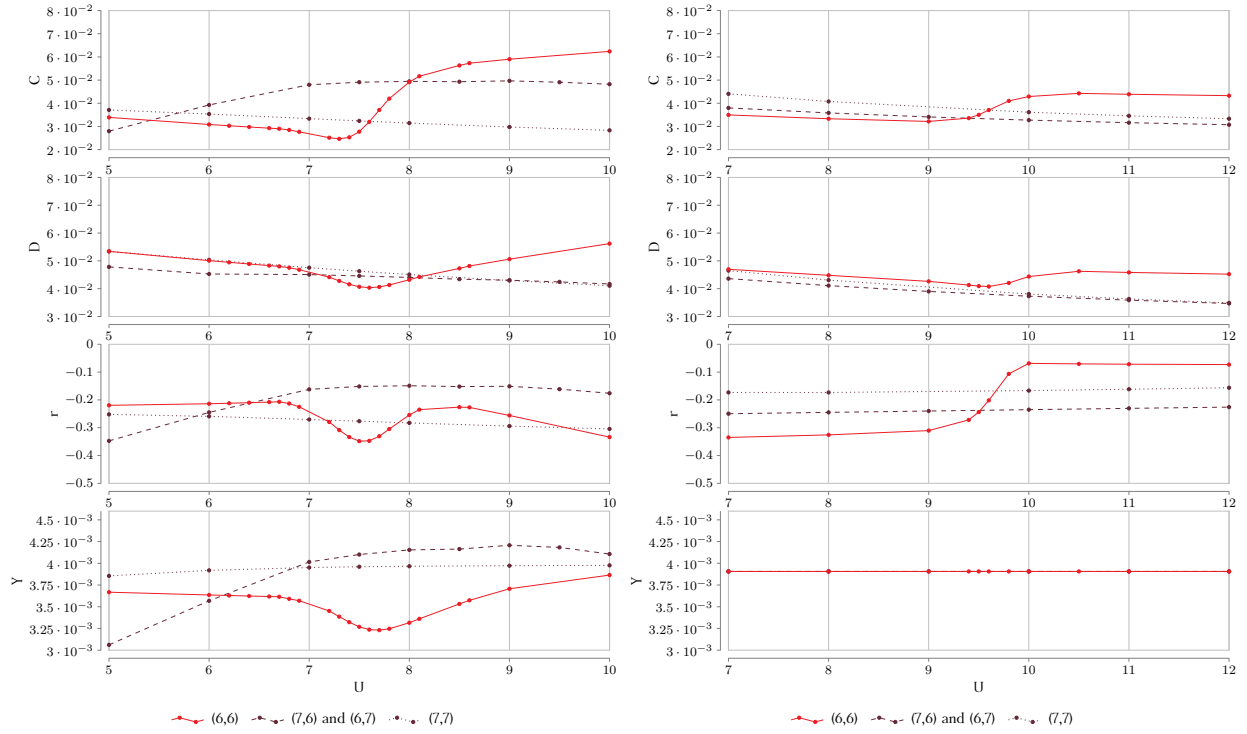


Figure 2: Characteristics of the mutual information complex network, – clustering C , density D , Pearson correlation r between neighboring sites in the middle of the 4-by-4 plaquette, and disparity Y of a site in the middle of the plaquette, – as functions of the on-site Coulomb repulsion U computed in different sectors for non-periodic (left panel) and periodic (right panel) boundary conditions. The hopping is $t'/t = -0.3$, the inverse temperature is $\beta = 100$.

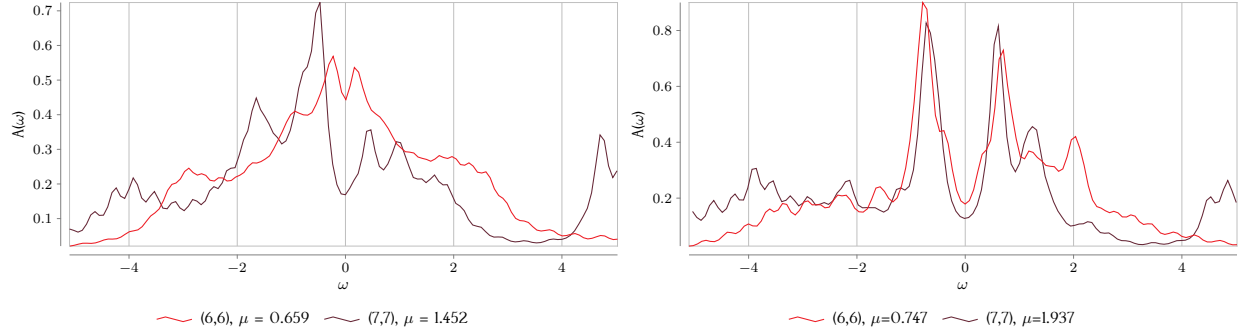


Figure 3: The density of states computed with non-periodic (left) and periodic boundary conditions. Whereas the comparison of different boundary shows that quantitatively the finite-size effects are important, qualitatively, in both schemes one can see the pseudogap formation near the quantum critical point. Its interpretation in terms of the Fano antiresonance due to formation of a “soft fermion” mode was given in Ref.¹¹

the complex network theory ($U = 7.5$, sector (6,6)) the peak in the d.o.s. starts splitting and the pseudogap emerges, see Fig. 3. Further decrease of the hole doping leads to enhancement of the gap. The particular role of U in this transition is less clear, as the d.o.s. profile varies very mildly upon changing U . The only peculiarity one can spot is that the emerged peaks become symmetric when passing the $U \simeq 7.5$ point in the (6,6) sector. However, since the d.o.s. for the other choice of boundary conditions do not reveal any specific features, it would be safer to claim that the low-order correlation functions are not sensitive to the discussed quantum phase transition. Ideologically, this situation is somewhat similar to the Anderson localization in disordered systems which is a clear example of a phenomenon that cannot be detected on the level of the average Green’s functions³⁹.

Discussion. By associating the quantum state of the $t-t'$ Hubbard model with a weighted network of inter-site mutual information, for different values of the next-neighbor hopping t'/t , we have found a transition point where characteristics of the network have a clearly distinguishable cusp. Such a behavior was previously shown to be an indication of a quantum phase transition in different one-dimensional models^{37,38}. Strikingly, this cusp is located exactly in the sector where onset of the pseudogap is expected to occur. The modern experimental understanding of the putative QCP in cuprates tells that it indeed must be associated with the emergence of the pseudogap phase¹⁵. Experimentally, for YBCO compounds the onset of pseudogap was demonstrated to happen at hole doping $\delta \simeq 22\%$ ⁴⁰. The hole doping $\delta = 25\%$ is the closest value one can get for a 4-by-4 cluster (the (6, 6) sector), and that's precisely the point where we observe the phase transition. The particular values of the on-site Coulomb doping is affected by the finite size effects, and estimated to be in the range $U \simeq 7 - 10$, dependent on the adopted boundary conditions. At the same time, no peculiarity is seen in the density of states at the transition point which might be a good indication that the low-order correlation functions that define the spectral and the response properties of the system could be blind to restructuring of many-body quantum states, and does not contain enough information on the role of quantum correlations behind phase transitions in electron systems.

Methods. In this section we give the relevant technical details of the calculation of the entanglement measures defined above. The first step is to diagonalize the Hubbard model (1) for a 4-by-4 cluster. This can be done either for a periodic or a non-periodic model. The diagonalization is performed using the Lanczos algorithm with 200 Krylov basis vectors⁴¹. The particle number and

spin conservation laws are used so that the diagonalization can be restricted to a sector with a fixed number of up- and down-spins. Those eigenstates with the corresponding eigenvectors are then used to calculate the reduced density matrices for each possible pair of sites as well as for each single site.

The reduced density matrix is computed using its definition that can be symbolically written as:

$$\rho_A(a, a') = \frac{1}{Z} \sum_n e^{-\beta E_n} \text{Tr}_{\bar{A}} |\psi_{n,(a,\bar{a})}\rangle \langle \psi_{n,(a',\bar{a})}|. \quad (8)$$

Here a, a' denote the many-particle (Fock) basis states describing the subsystem A we calculate the density matrix for, \bar{a} stands for the many-particle basis state of the complementary subsystem \bar{A} , thus a couple of those (a, \bar{a}) denotes a basis Fock state for the whole cluster explicitly split into two parts. As before, n stands for a particular eigenvector, the density matrices for given eigenstates are weighted with the Boltzmann factors corresponding to their energies. In a given sector for a given set of parameters we use the Boltzmann factor cut-off of 1% meaning $e^{(E_0 - E_i)\beta} > 10^{-2}$, where E_0 is the ground state energy and E_i is the energy of the highest (i th) level taken into account. Note that while performing the partial trace over \bar{A} one has to correctly account for the fermionic commutation relations. To this aim one has to effectively change the numeration of sites so that the sites for which we calculate the density matrix stand first. Explicitly it means that each component of an eigenvector, corresponding to a given basis state of the cluster, gets a factor determined as the parity acquired while "dragging" the occupied sites of A to the beginning past the occupied states of \bar{A} . In other words for each basis vector one takes each occupied site

from A and for each occupied spin component counts the number of same spin occupied sites from \bar{A} standing before the considered site in the original numeration. Summing up the parities of those numbers for all occupied sites and spins from A one gets the parity that is assigned to a given basis vector with respect to the subsystem A . Having multiplied the eigenvector components with the acquired parities one finally performs the partial trace over the complementary subset \bar{A} .

Given the reduced density matrix we first calculate the von Neumann entropy of a given subsystem and then, with (2) the mutual information for each pair of sites, that serves as the basis for our network.

The ω -dependent Green function is given by:

$$G_{i,\sigma}(\omega) = \frac{1}{Z} \sum_{m,n} \frac{|\langle m | c_{i,\sigma}^\dagger | n \rangle|^2}{\omega + E_n - E_m} (e^{-\beta E_n} + e^{-\beta E_m}). \quad (9)$$

Here m, n denote the eigenstates of the system, i and σ denote a given site and spin (in the paramagnetic case the answer is spin-independent), E_n is the energy of the n -th state, and $Z = \sum_m e^{-\beta E_m}$ is the partition function. Note that m and n necessarily belong to different sectors.

The Green function is used to calculate the density of states. The delta-peaks are broadened with $\delta = \pi/\beta$.

Acknowledgements. Authors thank Lincoln Carr for inspiring discussions.

Competing Interests. The Authors declare no Competing Financial or Non-Financial Interests.

Author contributions. A.A.B., M.I.K. and A.I.L. designed the project and directed it with the help of

S.B., M.D. and M.H. performed the calculations. A.A.B., M.I.K. and S.B. wrote the manuscript. All authors contributed to discussions.

Funding. A.A.B. and M.I.K. would like to thank the support of NWO via Spinoza Prize and of ERC Advanced Grant 338957 FEMTO/NANO.

Data Availability. The data that support the findings of this study are available from the corresponding author upon reasonable request.

1. P.W. Anderson, *The Theory of Superconductivity in the High- T_c Cuprates* (Princeton University Press, Princeton, 2007).
2. E. Dagotto, Correlated electrons in high-temperature superconductors, *Rev. Mod. Phys.* **66**, 763-840 (1994).
3. J. Orenstein, and A.J. Millis, Advances in the physics of high-temperature superconductivity, *Science* **288**, 468-474 (2000).
4. D.J. Scalapino, A common thread: The pairing interaction for unconventional superconductors, *Rev. Mod. Phys.* **84**, 1383-1417 (2012).
5. O.K. Andersen, A.I. Liechtenstein, O. Jepsen, F. Paulsen LDA energy bands, low-energy hamiltonians, t' , t'' , $t_{\perp}(k)$, and J_{\perp} , *Journal of Physics and Chemistry of Solids*, **56**, 1573–1591 (1995).
6. Th. Maier, M. Jarrell, Th. Pruschke, and M. H. Hettler, Quantum cluster theories, *Rev. Mod. Phys.* **77**, 1027 (2005)

7. K. Haule and G. Kotliar, Strongly correlated superconductivity: A plaquette dynamical mean-field theory study, *Phys. Rev. B* **76**, 104509 (2007)
8. E. Khatami, K. Mielson, D. Galanakis, A. Macridin, J. Moreno, R. T. Scalettar, and M. Jarrell, Quantum criticality due to incipient phase separation in the two-dimensional Hubbard model, *Phys. Rev. B* **81**, 201101(R) (2010)
9. E. Gull, O. Parcollet, and A. J. Millis, Superconductivity and the Pseudogap in the Two-Dimensional Hubbard Model, *Phys. Rev. Lett.* **110**, 216405 (2013)
10. M. Civelli, Evolution of the Dynamical Pairing across the Phase Diagram of a Strongly Correlated High-Temperature Superconductor, *Phys. Rev. Lett.* **103**, 136402 (2009)
11. M. Harland, M.I. Katsnelson, A.I. Lichtenstein Plaquette valence bond theory of high-temperature superconductivity, *Phys. Rev. B* **94**, 125133 (2016).
12. S. Sachdev, H.D. Scammell, M.S. Scheurer, and G. Tarnopolsky, Gauge theory for the cuprates near optimal doping, arXiv:1811.04930.
13. S. Sachdev, *Quantum Phase Transitions*, second edition (Cambridge University Press, Cambridge, 2011).
14. J.G. Bednorz and K.A. Müller, Possible high-T_c superconductivity in the BaLaCuO system, *Z. Phys. B: Condens. Matter* **64**, 189-193 (1986).
15. N.E. Hussey, J. Buhot, and S. Licciardello, A tale of two metals: contrasting criticalities in the pnictides and hole-doped cuprates, *Rep. Prog. Phys.* **81**, 052501 (2018).

16. B. Michon et al., Thermodynamic signatures of quantum criticality in cuprate superconductors, *Nature* **567**, 218222 (2019)
17. A.A. Abrikosov, L.P. Gorkov, and I.E. Dzialoshinski, *Methods of Quantum Field Theory in Statistical Physics* (Dover, New York, 1975).
18. G.D. Mahan, *Many-Particle Physics*, third edition (Springer, New York, 2000).
19. J. Maldacena, The large-N limit of superconformal field theories and supergravity, *Int. j. of theor. phys.* **38**, 1113–1133 (1999).
20. J. Zaanen, Y. Liu, Y.W. Sun, K. Schalm, *Holographic Duality in Condensed Matter Physics*, (Cambridge University Press, Cambridge, 2015).
21. S.A. Hartnoll, A. Lucas, and S. Sachdev, *Holographic Quantum Matter* (MIP Press, Cambridge Mass., 2018).
22. A. Legros et al., Universal T-linear resistivity and Planckian dissipation in overdoped cuprates, *Nature Physics* **15**, 142147 (2019)
23. R.A. Davison, K. Schalm, J. Zaanen, Holographic duality and the resistivity of strange metals, *Phys. Rev. B* **89**, 245116 (2014).
24. M. Blake, A. Donos, Quantum critical transport and the Hall angle in holographic models, *Phys. Rev. Lett.* **114**, 021601 (2015).
25. A. Donos, S. Hartnoll, Interaction-driven localization in holography, *Nature Physics* **9**, 649–655 (2013).

26. T. Andrade, A. Krikun, K. Schalm, J. Zaanen, Doping the holographic Mott insulator, *Nature physics* **14**, 1049–1055 (2018).
27. V.Y. Irkhin, A.A. Katanin, and M.I. Katsnelson, Effects of van Hove singularities on magnetism and superconductivity in the t - t' Hubbard model: A parquet approach, *Phys. Rev. B* **64**, 165107 (2001).
28. C.J. Halboth, W. Metzner, Renormalization-group analysis of the two-dimensional Hubbard model, *Phys. Rev. B* **61**, 7364–7377 (1999).
29. A. Neumayr, W. Metzner, Renormalized perturbation theory for Fermi systems: Fermi surface deformation and superconductivity in the two-dimensional Hubbard model, *Phys. Rev. B* **67**, 035112 (2003).
30. J. Reiss, D. Rohe, W. Metzner, Renormalized mean-field analysis of antiferromagnetism and d-wave superconductivity in the two-dimensional Hubbard model, *Phys. Rev. B* **75**, 075110 (2007).
31. A. Eberlein, W. Metzner, Superconductivity in the two-dimensional $t - t'$ -Hubbard model, *Phys. Rev. B* **89**, 035126 (2014).
32. M. Ossadnik, C. Honerkamp, T.M. Rice, and M. Sgrist, Breakdown of Landau Theory in Overdoped Cuprates near the Onset of Superconductivity, *Phys. Rev. Lett.* **101**, 256405 (2008).
33. A.I. Lichtenstein and M.I. Katsnelson, Antiferromagnetism and d-wave superconductivity in cuprates: A cluster dynamical mean-field theory, *Phys. Rev. B* **62**, R9283-R9286 (R) (2000).

34. H.C. Jiang, T.P. Devereaux, Superconductivity in the doped Hubbard model and its interplay with charge stripes and next-nearest hopping t' , arXiv: 1806.01465.
35. H.C. Jiang, Z.Y. Weng, S.A. Kivelson Superconductivity in the doped $t - J$ model: results for four-leg cylinders, *Phys. Rev. B* **98**, 140505 (2018).
36. E.W. Huang, R. Sheppard, B. Moritz, T.P. Devereaux, Strange metallicity in the doped Hubbard model, arXiv: 1806.08346.
37. M.A. Valdez, D. Jaschke, D.L. Vargas, L.D. Carr, Quantifying Complexity in Quantum Phase Transitions via Mutual Information Complex Networks, *Phys. Rev. Lett.* **119**, 225301 (2017).
38. B. Sundar, M.A. Valdez, L.D. Carr, K.R.A. Hazzard, A complex network description of thermal quantum states in the Ising spin chain, *Phys. Rev. A* **97**, 052320 (2018).
39. I.M. Lifshitz, S.A. Gredeskul, L.A. Pastur, *Introduction to the Theory of Disordered Systems* (Wiley, New York, 1988).
40. Y. Sato et al. Thermodynamic evidence for nematic phase transition at the onset of pseudogap in $\text{YBa}_2\text{Cu}_3\text{O}_y$, *Nature Physics* **13**, 1074-1078 (2017).
41. S. Iskakov, M. Danilov, Many-body physics, Exact diagonalization, Hubbard model, Anderson impurity model, *Comp. Phys. Commun.* **225**, 128 (2018).